© 2020. Published by The Company of Biologists Ltd | Development (2020) 147, dev192161. doi:10.1242/dev.192161

STEM CELLS AND REGENERATION

RESEARCH ARTICLE

Endocannabinoid signalling in stem cells and cerebral organoids drives differentiation to deep layer projection neurons via CB_1 receptors

Juan Paraíso-Luna[1,2], José Aguareles[1,2], Ricardo Martín[2], Ane C. Ayo-Martín[3,4], Samuel Simón-Sánchez[1,2], Daniel García-Rincón[1,2], Carlos Costas-Insua[1,2], Elena García-Taboada[1,2], Adán de Salas-Quiroga[1,2,*], Javier Díaz-Alonso[1,2,‡], Isabel Liste[5], José Sánchez-Prieto[2], Silvia Cappello[3], Manuel Guzmán[1,2] and Ismael Galve-Roperh[1,2,§]

ABSTRACT

The endocannabinoid (eCB) system, via the cannabinoid CB_1 receptor, regulates neurodevelopment by controlling neural progenitor proliferation and neurogenesis. CB_1 receptor signalling *in vivo* drives corticofugal deep layer projection neuron development through the regulation of BCL11B and SATB2 transcription factors. Here, we investigated the role of eCB signalling in mouse pluripotent embryonic stem cell-derived neuronal differentiation. Characterization of the eCB system revealed increased expression of eCB-metabolizing enzymes, eCB ligands and CB_1 receptors during neuronal differentiation. CB_1 receptor knockdown inhibited neuronal differentiation of deep layer neurons and increased upper layer neuron generation, and this phenotype was rescued by CB_1 re-expression. Pharmacological regulation with CB_1 receptor agonists or elevation of eCB tone with a monoacylglycerol lipase inhibitor promoted neuronal differentiation of deep layer neurons at the expense of upper layer neurons. Patch-clamp analyses revealed that enhancing cannabinoid signalling facilitated neuronal differentiation and functionality. Noteworthy, incubation with CB_1 receptor agonists during human iPSC-derived cerebral organoid formation also promoted the expansion of $BCL11B^+$ neurons. These findings unveil a cell-autonomous role of eCB signalling that, via the CB_1 receptor, promotes mouse and human deep layer cortical neuron development.

KEY WORDS: Cortical development, Endocannabinoids, Neurogenesis, Projection neuron, Tetrahydrocannabinol, 2-Arachidonoylglycerol, Cerebral organoid

[1]Instituto Ramón y Cajal de Investigación Sanitaria (IRYCIS) and Centro de Investigación Biomédica en Red sobre Enfermedades Neurodegenerativas (CIBERNED), 28049 Madrid, Spain. [2]Department of Biochemistry and Molecular Biology, Complutense University, Instituto Universitario de Investigación en Neuroquímica (IUIN), 28040 Madrid, Spain. [3]Max Planck Institute of Psychiatry, 80804 Munich, Germany. [4]International Max Planck Research School for Translational Psychiatry (IMPRS-TP), 80804 Munich, Germany. [5]Unidad de Regeneración Neural, Unidad Funcional de Investigación de Enfermedades Crónicas (UFIEC), Instituto de Salud Carlos III (ISCIII), 28220 Madrid, Spain.

*Present address: Champalimaud Centre for the Unknown, 1400-038 Lisbon, Portugal. ‡Present address: Department of Anatomy and Neurobiology, University of California, Irvine, CA 92617, USA.

§Author for correspondence (igr@quim.ucm.es)

I.G.-R., 0000-0003-3501-2434

Handling Editor: François Guillemot
Received 28 April 2020; Accepted 3 November 2020

INTRODUCTION

Cannabinoids, the active molecules of the *Cannabis* plant, and particularly the most abundant and potent of them, Δ^9-tetrahydrocannabinol (THC), exert a wide variety of neuropsychiatric and neurological actions by impacting on the prominent neuromodulatory role of presynaptic cannabinoid CB_1 receptors (Cristino et al., 2020). Hence, deregulated expression and function of endocannabinoid (eCB) system elements (namely, eCB ligands, eCB receptors and eCB metabolic enzymes of synthesis and degradation; Fig. 1A) in different neural cell populations contribute to the complex role of this endogenous signalling system in neurodevelopmental psychiatric disorders (Sagredo et al., 2018), neurodegenerative diseases (Cristino et al., 2020) and the regulation of social behaviours and emotions (Wei et al., 2017). The neurodevelopmental function of the eCB system is evidenced by its ability to control fundamental processes such as neural progenitor proliferation, neuronal differentiation and migration, axonal guidance and circuit formation (Galve-Roperh et al., 2013; Maccarrone et al., 2014). Thus, embryonic development is an extremely sensitive period in which exposure to cannabinoids can induce remarkable disturbances of endogenous cannabinoid signalling (Scheyer et al., 2019). CB_1 receptors regulate long-range corticofugal neural projection development (Mulder et al., 2008; Wu et al., 2010; Díaz-Alonso et al., 2012). Particularly, during projection neuron differentiation, CB_1 receptor signalling controls the generation of layer V subcerebral projection neurons (Díaz-Alonso et al., 2012; de Salas-Quiroga et al., 2015). The eCB system also regulates the development and morphogenesis of GABAergic interneurons (Berghuis et al., 2005), and prenatal exposure to THC or synthetic cannabinoid receptor agonists induces a selective interneuronopathy with decreased hippocampal cholecystokinin-positive basket cell generation and long-lasting alterations of neurotransmission and behaviour (Vargish et al., 2016; de Salas-Quiroga et al., 2020). In addition, interfering with endogenous cannabinoid signalling, as induced by prenatal THC exposure, leads to a subcortical hyperdopaminergic state and alterations of noradrenergic signalling (Renard et al., 2017; Frau et al., 2019). Overall, interfering with CB_1 receptor signalling during embryonic development exerts profound changes in neuronal populations and network establishment. However, the cellular mechanisms responsible for these plastic adaptations remain largely unknown. In this sense, whereas *in vivo* studies have shown a consistent role of CB_1 receptor signalling in pyramidal neuron differentiation (Díaz-Alonso et al., 2012; de Salas-Quiroga et al., 2015), the interpretation of these observations is complex and

Development (2020) 147, dev192161. doi:10.1242/dev.192161

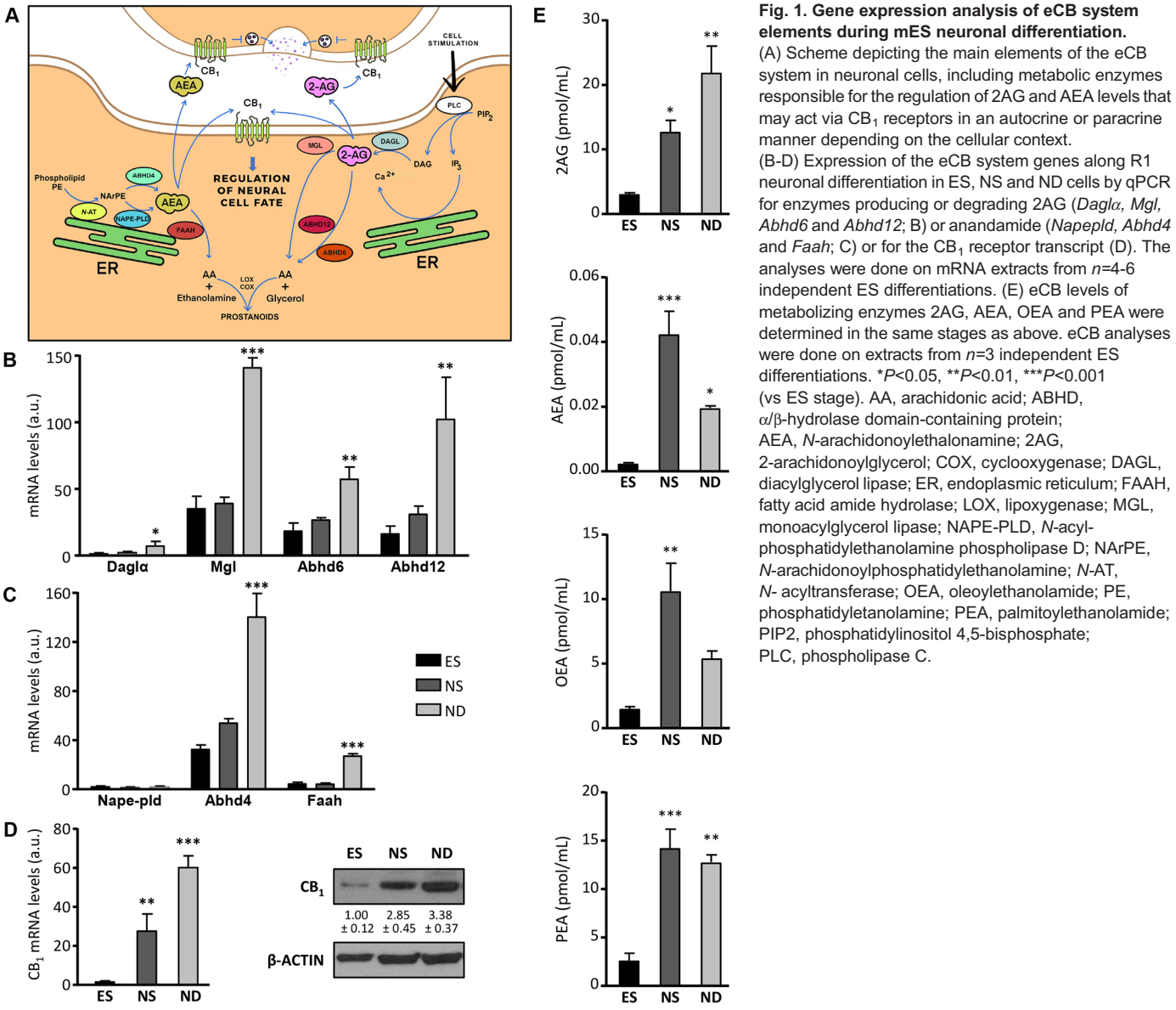

Fig. 1. Gene expression analysis of eCB system elements during mES neuronal differentiation. (A) Scheme depicting the main elements of the eCB system in neuronal cells, including metabolic enzymes responsible for the regulation of 2AG and AEA levels that may act via CB_1 receptors in an autocrine or paracrine manner depending on the cellular context. (B-D) Expression of the eCB system genes along R1 neuronal differentiation in ES, NS and ND cells by qPCR for enzymes producing or degrading 2AG (*Daglα, Mgl, Abhd6* and *Abhd12*; B) or anandamide (*Napepld, Abhd4* and *Faah*; C) or for the CB_1 receptor transcript (D). The analyses were done on mRNA extracts from n=4-6 independent ES differentiations. (E) eCB levels of metabolizing enzymes 2AG, AEA, OEA and PEA were determined in the same stages as above. eCB analyses were done on extracts from n=3 independent ES differentiations. *P<0.05, **P<0.01, ***P<0.001 (vs ES stage). AA, arachidonic acid; ABHD, α/β-hydrolase domain-containing protein; AEA, *N*-arachidonoylethalonamine; 2AG, 2-arachidonoylglycerol; COX, cyclooxygenase; DAGL, diacylglycerol lipase; ER, endoplasmic reticulum; FAAH, fatty acid amide hydrolase; LOX, lipoxygenase; MGL, monoacylglycerol lipase; NAPE-PLD, *N*-acyl-phosphatidylethanolamine phospholipase D; NArPE, *N*-arachidonoylphosphatidylethanolamine; *N*-AT, *N*- acyltransferase; OEA, oleoylethanolamide; PE, phosphatidyletanolamine; PEA, palmitoylethanolamide; PIP2, phosphatidylinositol 4,5-bisphosphate; PLC, phospholipase C.

makes it difficult to discriminate between cell-autonomous and non-cell-autonomous actions (Díaz-Alonso et al., 2015). Hence, in the present study we sought to characterize the cell-autonomous role of the eCB system in embryonic stem cell-derived neuronal differentiation, as well as the consequences of its pharmacological or genetic manipulation.

Our data show that the eCB system maturates in parallel with neuronal differentiation, regulating pyramidal neuron differentiation via CB_1 receptor signalling. Specifically, CB_1 receptor knockdown inhibits layer V neuronal differentiation. In addition, pharmacological regulation with the monoacylglycerol lipase (MGL) inhibitor JZL-184 and the cannabinoid receptor agonists THC and HU-210 exert an opposite action and increase the generation of deep layer pyramidal neurons, at the expense of upper layer pyramidal neurons, by modulating the activity of BCL11B and SATB2 transcription factors. These findings support a cell-autonomous role for eCB signalling and contribute to our understanding of the neurobiological impact of embryonic cannabinoid exposure and the associated risk of developing neuropsychiatric alterations and neurodevelopmental disorders.

RESULTS

The eCB system is induced during ES cell-derived default neuronal differentiation

After neural induction, R1 mouse embryonic stem (mES) cells were differentiated in a chemically defined medium that contained no morphogens and in the presence of the sonic hedgehog inhibitor cyclopamine (Gaspard et al., 2008). The expression of pluripotency, neural stem and neural differentiation markers was monitored by real time quantitative PCR (qPCR) and immunofluorescence to follow ES transition to neural stem (NS) and neural differentiated (ND) cells. Neuronal differentiation was reflected by the induction of markers TUJ1 and NeuN, concomitant with the disappearance of pluripotency markers and the NS marker nestin (Fig. S1A). Transient expression of *Pax6* and *Tbr2* was observed during the NS stage. Gene expression analysis of dorsal telencephalic neuronal identity marker transcripts (*Tbr1*, *Bcl11b*, *Er81*, *Uchl1*, *Cux2* and *Satb2*) indicated a developmentally regulated gene expression profile (Fig. S1B). After differentiation most cells were neurons, as indicated by TUJ1 and NeuN expression. Immunofluorescence for vGLUT1 combined with vGAT1, or glutamate and GABA, revealed that most

Development (2020) 147, dev192161. doi:10.1242/dev.192161

differentiated cells were excitatory glutamatergic neurons (79.1±4.6% TUJ1$^+$vGLUT1$^+$ cells, n=4; Fig. S1C,D). ES-derived projection neurons showed expression of laminar markers characteristic of deep and upper layer neurons (i.e. BCL11B$^+$ and Satb2$^+$ neurons, respectively) (Fig. S1E). Reaching final differentiation, cells expressing one or the other marker did not co-express both proteins as they are usually mutually exclusive when fully differentiated (Greig et al., 2013). Furthermore, ES-derived neurons were functional, as determined by patch-clamp studies (Fig. S1F), firing action potentials in response to injected currents from 30 pA, which is consistent with early stages of pyramidal neurons from layer V of the mouse cerebral cortex (Zhang, 2004; Kroon et al., 2019). The neuronal identity of patched cells was confirmed by immunofluorescence with an anti-ER81 antibody in biocytin-labelled cells (Fig. S1G).

To characterize the development of the eCB system during mES neuronal differentiation, we performed qPCR gene expression analysis of the different eCB metabolizing enzymes. Fig. 1A illustrates the subcellular localization of the major eCB-synthesizing and eCB-degrading enzymes, as well as the mechanism of eCB action via CB_1 receptors. The 2-arachidonoylglycerol (2AG)-synthesizing enzyme diacylglycerol lipase α (*Daglα*, recommended name *Dagla*) increased with neural differentiation (Fig. 1B), whereas transcripts of the 2AG-degrading enzyme monoacylglycerol lipase (*Mgl*) were equivalent in ES and NS cells, and its levels increased thereafter with neuronal differentiation. The expression of other 2AG-degrading enzymes, α/β-hydrolase domain-containing proteins 6 and 12 (*Abhd6* and *Abhd12*), also increased at the ND stage. The *Daglβ* (recommended name *Daglb)* isoform increased with neural differentiation, similarly to *Daglα* (ES, NS and ND levels were 1.00±0.16, 4.05±0.47 and 7.41±0.26, respectively; **P=0.0068 ES vs NS; ***P=0.0008 ES vs ND). The expression of the *N*-arachidonoylethalonamine (AEA)-synthesising enzyme *N*-acylphosphatidylethanolamine phospholipase D *(Napepld)* was low at all the stages analysed; *Abhd4* steadily increased along ES default differentiation, whereas the AEA-degrading enzyme fatty acid amide hydrolase (*Faah*) reached higher levels in ND cells (Fig. 1C). In concert with the maturation of a functional eCB system, we observed cannabinoid CB_1 receptor upregulation. CB_1 receptor transcript and protein levels were induced during the transition from ES to multipotent NS cells and further increased along neural differentiation (Fig. 1D). Next, eCB levels were determined during ES neural differentiation. 2AG levels increased steadily and reached higher values at the ND stage, whereas the levels of the *N*-acylethanolamines AEA, OEA and PEA were higher at the NS state (Fig. 1E). Immunofluorescence characterization confirmed the presence of CB_1 receptors in pluripotent R1 cells that co-express OCT4, as well as its presence in nestin$^+$ NS cells and TUJ1$^+$ neurons (Fig. 2A). At more differentiated states, CB_1 receptor expression was evident in BCL11B$^+$ deep layer neurons (Fig. 2B). Representative microscopy images evidence the expression of DAGL-α, MGL, NAPE-PLD and FAAH in ES-derived nestin$^+$ NS cells and TUJ1$^+$ neurons (ND), thus confirming the maturation of the eCB system along neuronal differentiation (Fig. 2C,D). In summary, these data demonstrate that mES cell-derived pyramidal neuronal differentiation is accompanied by the acquisition of a functional eCB signalling system.

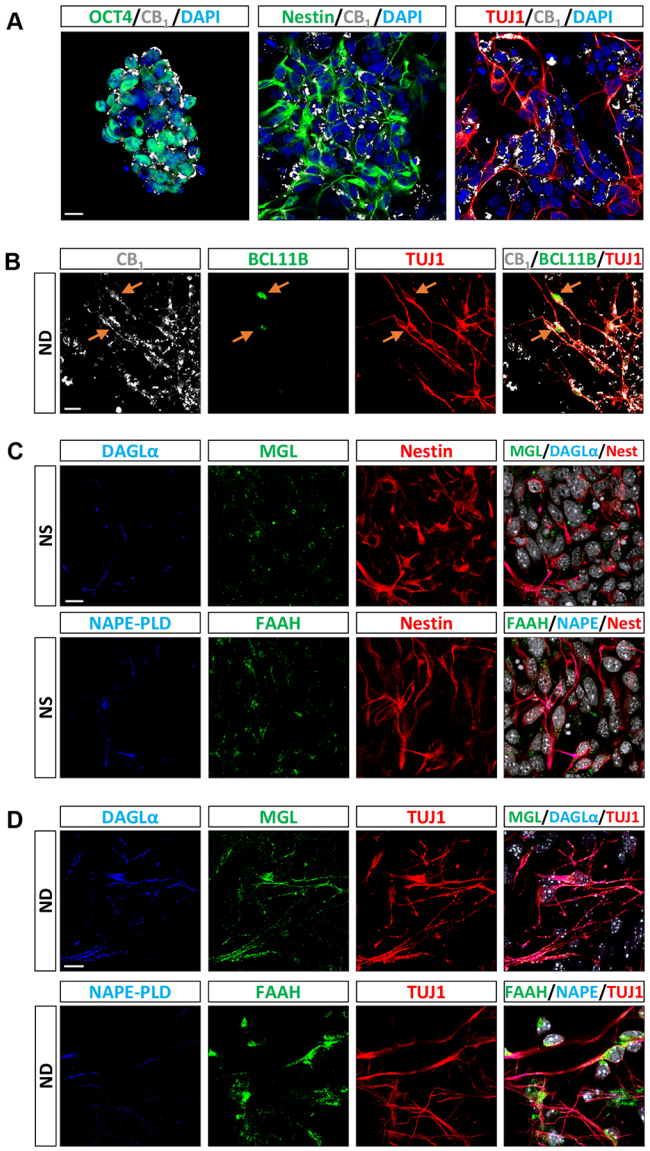

Fig. 2. Characterization of CB_1 receptor expression and eCB-metabolizing enzymes during mES cell differentiation. (A) CB_1 receptor expression was analysed by immunofluorescence in ES, NS and ND cells together with specific markers for each stage, OCT4, nestin and TUJ1, respectively, with specific antibodies. Representative images are shown. (B) CB_1 receptor expression immunofluorescence in deep layer neurons co-labelled with anti-BCL11B and anti-TUJ1 antibodies. (C,D) Immunofluorescence characterization for DAGLα, MGL and NAPE-PLD, FAAH expression in ES-derived nestin$^+$ NS cells and TUJ1$^+$ neurons (at NS and ND stages). Arrows indicate BCL11B$^+$ cells. Scale bars: 10 µm (A,C,D); 25 µm (B).

CB_1 receptor signalling promotes deep layer neuronal differentiation

We assessed the impact of CB_1 receptor ablation in mES-derived neuronal differentiation by using a short-hairpin (sh) RNA knockdown strategy. Western blot analysis showed the efficacy of shCB$_1$-mediated knockdown at the protein level (Fig. S2A). Functional confirmation of CB_1 receptor ablation was demonstrated by the loss of HU-210-induced extracellular signal-regulated kinase (ERK) activation (phosphorylation) as determined by western blot analyses of shControl-transfected and shCB$_1$-transfected R1 mES-derived cells (referred to here as shCtrl-R1 and shCB$_1$-R1 cells, respectively) [shCtrl-R1, vehicle (1.00±0.40) vs HU-210 (1.78±0.19), *P=0.015; shCB$_1$-R1, vehicle (1.00±0.20) vs HU-210 (0.98±0.07), P=0.759; n=4]. Quantification of neuronal populations was performed in CB_1 receptor knockdown ES-derived neurons (neurons derived from shCB$_1$-R1 cells) after

Development (2020) 147, dev192161. doi:10.1242/dev.192161

immunofluorescence and showed inhibited deep layer neuronal differentiation, as evidenced by decreased BCL11B$^+$, ER81$^+$ neurons and increased SATB2$^+$ upper layer neurons (Fig. 3A,B). Gene expression analyses showed that CB_1 receptor knockdown reduced *Bcl11b* and *Er81* mRNA levels, with a concomitant increase in the upper layer neuronal markers *Satb2* and *Cux2* (Fig. 3C). To evaluate the specificity of shRNA-mediated CB_1 receptor knockdown we performed genetic rescue experiments, transfecting shCtrl-R1 and shCB_1-R1 cells with a CB_1 expression plasmid that is not recognized by the shCB_1 sequence. CB_1 receptor expression rescue, as shown at the mRNA and protein level (Fig. S2B-D), restored the ability of THC to induce ERK activation (Fig. S2E). Importantly, CB_1 receptor rescue reversed the consequences of CB_1 loss of function, thus increasing BCL11B$^+$, ER81$^+$ neuronal differentiation and decreasing SATB2$^+$ cells (Fig. 3A-C). We further proved the cell-autonomous action of CB_1 receptors in deep layer neuronal differentiation by transfecting shCB_1 and shCtrl R1-derived NS cells, with subsequent colocalization analyses of CB_1 receptor and the BCL11B and SATB2 identity markers in transfected GFP$^+$ cells, as well as immunoreactive-area analyses for both markers in GFP$^+$ cells (Fig. S3A-E). Consequently, in shCB_1-R1 derived GFP$^+$ cells, CB_1 receptors and BCL11B cells were not expressed, but SATB2 was present. In summary, these results demonstrate a cell-autonomous role of CB_1 receptor signalling in deep layer pyramidal differentiation.

Increased eCB tone drives deep layer pyramidal neuronal differentiation via CB_1 receptors

To assess the involvement of endogenous cannabinoid tone in ES-derived neuronal differentiation, we characterized the neuronal populations generated under pharmacological MGL inhibition. Treatment with JZL-184 (1 µM) during ES differentiation from 14 to 21 days in vitro (DIV), every two days, increased 2AG levels as well as those of the other major eCB, AEA (Fig. S4A). The presence of a high eCB tone increased neuronal differentiation towards the generation of deep layer projection neurons, identified by the expression of BCL11B and ER81 (Fig. 4A,B). In concert, JZL-184 treatment decreased the SATB2$^+$ neuronal population. To determine the role of CB_1 receptors mediating JZL-184-derived eCB-driven regulation of neurogenesis, we determined the impact of co-incubation with the CB_1 inverse agonist AM-251, which effectively prevented JZL-184 consequences in neuronal differentiation

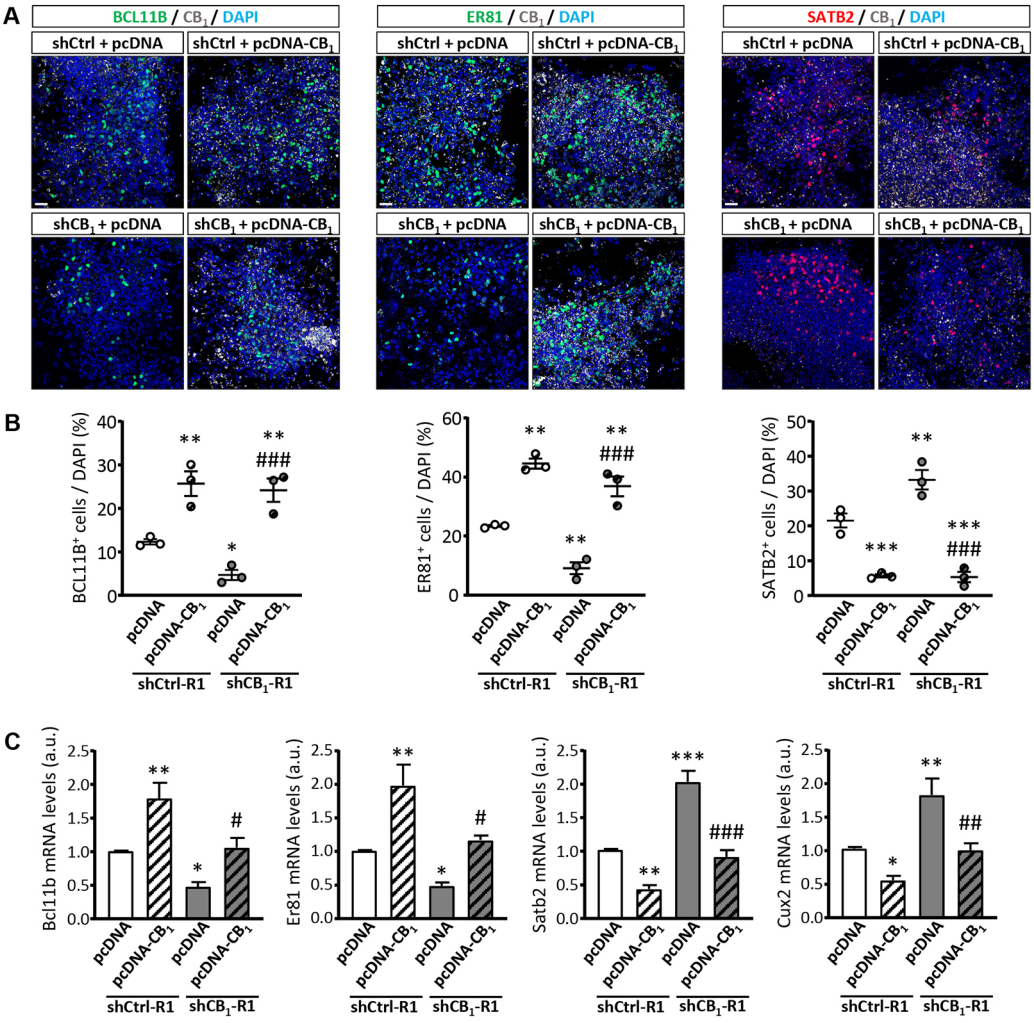

Fig. 3. CB_1 receptors promote ES cell differentiation in deep cortical neurons. (A,B) Representative images and quantification of BCL11B$^+$, ER81$^+$ and SATB2$^+$ cells in ND cells derived from shCtrl-R1 and shCB_1-R1 cells. CB_1 receptor expression rescue was performed by transfection with control and hCB_1-pcDNA plasmids. (C) qPCR quantification of *Bcl11b, Er81, Satb2* and *Cux2* mRNA levels in ND cells differentiated as above. (A,B) The analyses were done on cells from *n*=3 independent ES differentiations. (C) The analyses were done on mRNA extracts from *n*=4 independent ES differentiations. **P*<0.05, ***P*<0.01, ****P*<0.001 (vs shCtrl-R1+pcDNA); $^{\#}P$<0.05, $^{\#\#}P$<0.01, $^{\#\#\#}P$<0.001 (vs shCB_1+pcDNA). Scale bar: 25 µm.

Development (2020) 147, dev192161. doi:10.1242/dev.192161

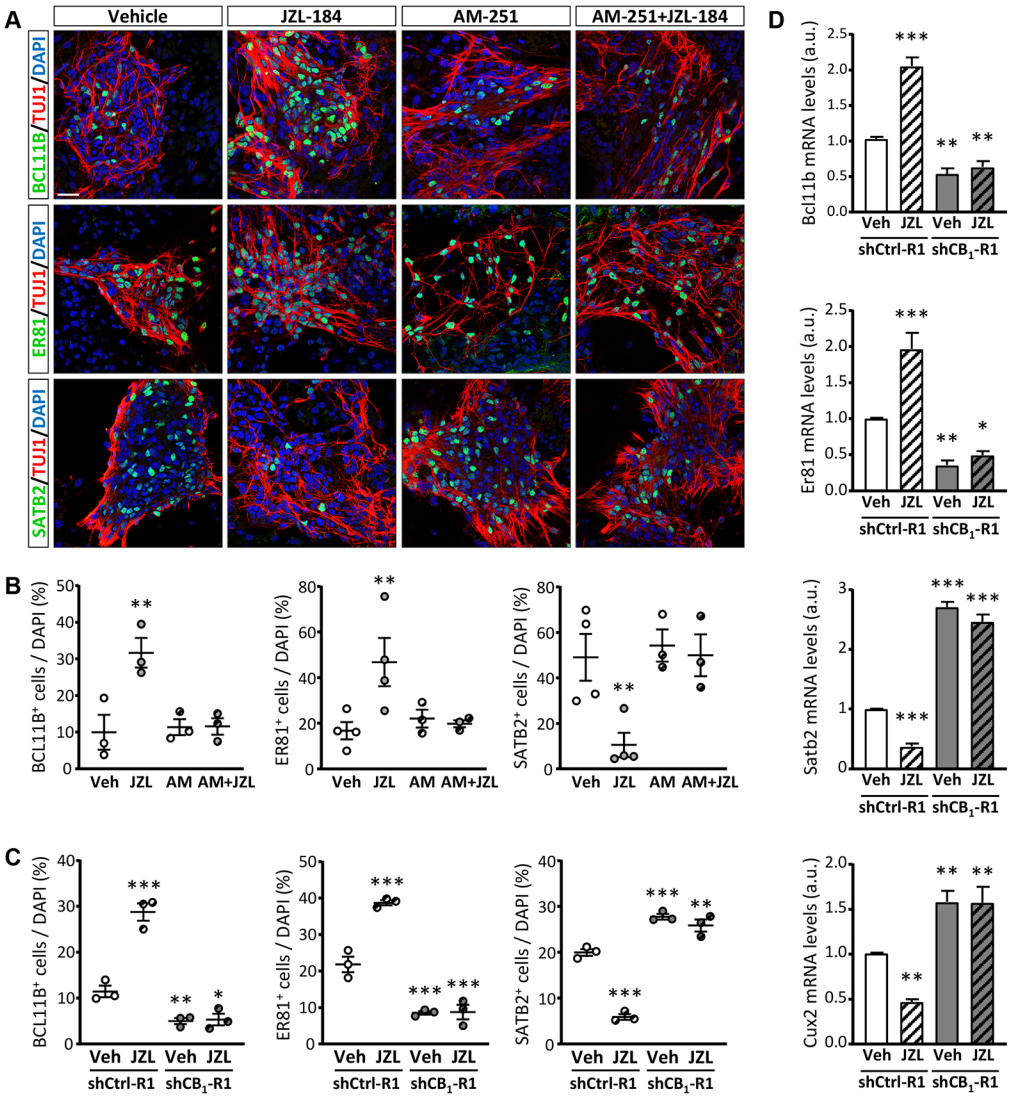

Fig. 4. Monoacylglycerol lipase inhibition by JZL-184 favours deep layer pyramidal neuron differentiation. (A) R1 cells were differentiated in the presence of THC (2 µM) in the absence or presence of AM-251 (1 µM). Representative immunofluorescence images are shown after BCL11B, ER81, SATB2 and TUJ1 immunofluorescence. (B) Quantification of BCL11B$^+$, ER81$^+$ and SATB2$^+$ cells in cannabinoid-differentiated neurons (as above) compared with vehicle-treated cells. (C) Quantification of BCL11B$^+$, ER81$^+$ and SATB2$^+$ cells in JZL-184-treated differentiating neurons derived from shCtrl-R1 and shCB$_1$-R1 cells. (D) Gene expression analyses of *Bcl11b, Er81, Satb2* and *Cux2* was performed at ND stage by qPCR in cell extracts as above. (B,C) The analyses were done on cells from *n*=3-4 independent ES differentiations. (D) The analyses were done on mRNA extracts from *n*=3 independent ES differentiations. **P*<0.05, ***P*<0.01, ****P*<0.001 (vs vehicle in shCtrl-R1 cells). Scale bar: 25 µm.

(Fig. 4A,B). Moreover, in ES cells deficient in CB$_1$ receptors (shCB$_1$-R1 cells), JZL-184 treatment was ineffective at inducing BCL11B$^+$, increasing ER81$^+$ neurons or decreasing SATB2$^+$ cells, whereas these effects were evident in shCtrl-R1 cells (Fig. 4C; Fig. S4B). This effect was also observed in shCB$_1$- and shCtrl-transfected R1-derived NS cells (Fig. S4C). Gene expression analyses confirmed neuronal population immunofluorescence studies by showing that JZL-184 increased mRNA levels of *Bcl11b* and *Er81* and decreased those of *Satb2* and *Cux2* in a CB$_1$ receptor-dependent manner (Fig. 4D). Thus, inhibition of 2AG degradation by JZL-184 pharmacological regulation promotes deep layer neuronal differentiation via CB$_1$ receptor signalling.

THC promotes deep layer neuronal differentiation via CB$_1$ receptors

Given the evidence for the role of CB$_1$ receptors in neuronal differentiation *in vivo* (Mulder et al., 2008; Díaz-Alonso et al., 2012; de Salas-Quiroga et al., 2015), we next characterized the impact of CB$_1$ receptor signalling by direct pharmacological manipulation. In R1 cells challenged with the CB$_1$ agonist HU-210 (100 nM), HU-210 reduced nestin-positive NS cells and increased the number of TUJ1$^+$, TBR1$^+$ cells in a CB$_1$ receptor-dependent manner. The effect was reversed by co-incubation with CB$_1$ receptor antagonist AM-251 (1 µM) (Fig. S5A-C; Table S1). In agreement, NeuN$^+$ mature neurons increased in the presence of HU-210 (Fig. S5D; Table S1). Quantification of TUJ1 immunofluorescence images indicated that ES-derived neurons that differentiated in the presence of HU-210 had an increase in the length of their main neurite (101.8±12.8 µm in HU-210-treated vs 50.1±4.9 µm in vehicle-treated ES-derived neurons; ***P*=0.0054). We then determined the impact of THC (2 µM) on neuronal differentiation. THC presence during ES neuronal differentiation favoured deep layer neuronal differentiation, as indicated by increased generation of BCL11B$^+$ and ER81$^+$ neurons at the expense of SATB2$^+$ upper layer neurons (Fig. 5A,B). THC and HU-210 pro-neurogenic action was confirmed by gene expression analyses, and increased *NeuN* mRNA levels were prevented by AM-251, hence confirming a CB$_1$ receptor-dependent mechanism (Fig. S5E). Likewise, both cannabinoid ligands, HU-210 and THC, increased transcript levels of the deep layer neuronal determinants *Bcl11b* and *Er81*, while decreasing upper layer *Satb2* and *Cux2* transcript levels (Fig. S5E). As an additional analysis of the status of the BCL11B/SATB2-regulated neuronal identity program, we examined the expression of netrin1 axon guidance receptors *Unc5C* and deleted in colorectal cancer (*Dcc*), which are involved in axonal guidance of corticofugal and callosal projection neurons, respectively (Srivatsa

Development (2020) 147, dev192161. doi:10.1242/dev.192161

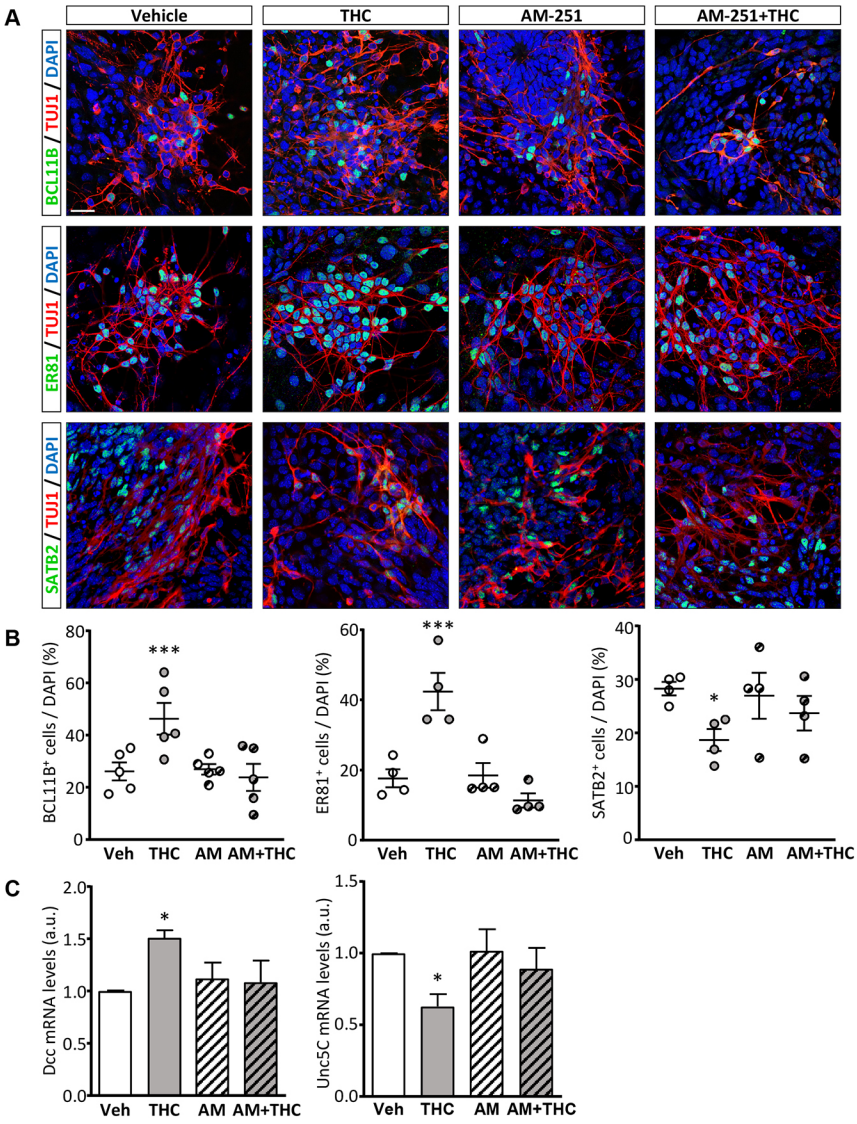

Fig. 5. THC favours deep layer pyramidal neuron differentiation. (A) R1 cells were differentiated in the presence of THC (2 µM) in the absence or presence of AM-251 (1 µM) or vehicle. Representative immunofluorescence images are shown after BCL11B, ER81, SATB2 and TUJ1 immunofluorescence. (B) Quantification of BCL11B$^+$, ER81$^+$ and SATB2$^+$ cells in cannabinoid-differentiated neurons (as above) compared with vehicle-treated cells. (C) Gene expression analyses of *Dcc* and *Unc5C* was performed at ND stage by qPCR. The analyses were done in cells (A,B) and mRNA extracts (C) from *n*=4-5 independent ES differentiations. **P*<0.05, ****P*<0.001 (vs vehicle). Scale bar: 25 µm.

et al., 2014). We found that neurons generated in the presence of THC exhibited increased expression of *Dcc* transcripts and reduced expression of *Unc5C*, and this was a CB_1 receptor-mediated action (Fig. 5C).

CB_1 receptor regulation of *Bcl11b* depends on ERK and Akt signalling

Next, we sought to investigate the intracellular signalling mechanisms responsible for CB_1 receptor regulation of *Bcl11b* transcriptional activity and neuronal differentiation. Luciferase transcriptional assays in R1 cells exposed to THC showed that CB_1 receptor activation increased MAR-A4 transcriptional activity of the *Bcl11b* locus (Alcamo et al., 2008) as well as MAR1 transcriptional activity of the *Dcc* locus (Fig. S6A) (Srivatsa et al., 2014). Both effects were reversed by co-incubation with the CB_1 receptor antagonist AM-251. Likewise, JZL-184 increased transcriptional activity of the *Bcl11b* and *Dcc* loci in a CB_1 receptor-dependent manner (Fig. S6B). Next, we performed transcriptional assays in the HiB5 neural cell line. HiB5 cells treated with HU-210 showed increased MAR-A4 *Bcl11b* transcriptional activity, and this effect was partially counteracted by the overexpression of SATB2, indicating appropriate regulation of the transcriptional identity program (Alcamo et al., 2008). Moreover, HU-210-induced *Bcl11b* transcriptional activity was prevented by the presence of SKI alone and together with SATB2, whose interaction regulates transcriptional mechanisms of callosal neuron differentiation (Baranek et al., 2012) (Fig. S6C). Next, we assessed which CB_1 receptor downstream signalling pathways (Galve-Roperh et al., 2013) were involved in *Bcl11b* regulation by co-incubation with selective inhibitors of the extracellular signal-regulated kinase (ERK) pathway (UO126, 1 µM), Akt (Akti X, 2.5 µM), mTORC1 (rapamycin, 100 nM) and c-Jun N-terminal kinase (SP600125, 12.5 µM), as well as with a dibutyryl-cyclic AMP analogue (2.5 µM) (Fig. S6D). CB_1 receptor-induced *Bcl11b*-luciferase activity was dependent on the ERK and Akt pathways, but was independent of the mTORC1 pathway, JNK signalling and cAMP levels. Considering previous evidence that CB_1 receptor signalling can modulate protein levels by influencing the proteasome degradation pathway (Díaz-Alonso et al., 2017; Miller et al., 2018), we also evaluated the impact of proteasome inhibition by the MG-132 compound in CB_1 receptor regulation of *Bcl11b* activation. Treatment with MG-132 was ineffective in HU-210-induced *Bcl11b*-transcriptional activity, suggesting that regulation of proteostasis does not play a major role in CB_1 receptor regulation

Development (2020) 147, dev192161. doi:10.1242/dev.192161

of *Bcl11b* transcriptional activity. In summary, these data demonstrate that CB_1 receptor regulation of *Bcl11b*-driven deep layer pyramidal neuron differentiation is mediated by ERK and Akt signalling, but is independent of the regulation of cAMP, mTORC1 and JNK pathways, and of proteasomal degradation.

Differentiation in the presence of THC and JZL-184 favours neuronal maturation and activity

To further characterize the role of CB_1 receptor activity during neuronal differentiation, we determined the electrophysiological properties of vehicle- and THC-treated neurons by patch-clamp analyses. In current-clamp analyses, ES-derived neurons generated in the presence of THC showed lower action potential threshold (THC-derived neurons, −17.1±1.4 mV, n=44 cells vs vehicle-derived neurons, −10.4±1.2 mV, n=42 cells from n=4 independent differentiations; ***P=0.0004) and higher action potential amplitude (THC-derived neurons, 27.6±2.6 mV, n=44 vs vehicle-differentiated cells, 11.8±1.1 mV, n=42, ***P<0.0001) (Fig. 6A,C), getting closer to the values of these parameters at more mature stages of layer V pyramidal neurons (Zhang, 2004; Kroon et al., 2019). Furthermore, in voltage-clamp recordings we found that inward currents were also higher in THC-treated versus vehicle-treated neurons (THC-derived neurons at −10 mM, 1223.0±106.3 pA, n=44 vs vehicle-differentiated cells, 487.1±106.6 pA, n=42; ***P<0.0001) (Fig. 6B,C). Similar findings were observed in JZL-184-differentiated ES-derived neurons (Fig. 6D-F) (JZL-148 versus vehicle for differentiated neuron action potential threshold, −21.3±1.4 mV, n=41 cells vs −12.4±1.5 mV, n=29 cells from n=3 independent differentiations, ***P<0.0001; for action potential amplitude, 24.1±2.1 mV, n=41 cells vs 13.3±1.2 mV, n=29 cells, ***P<0.0001; for inward current, 814.9±58.2 pA, n=41 cells vs 545.6±72.3, n=29 cells, **P=0.0047). In summary, these data indicate that pharmacological regulation of CB_1 receptor signalling during ES-derived neuronal differentiation promotes cell functional maturation.

CB_1 receptor regulation of human iPS cell-derived organoids increases deep layer neuronal generation

To expand the implications of our findings demonstrating the role of CB_1 receptor signalling in deep layer neuronal differentiation, we moved to human induced pluripotent stem (hiPS) cell-derived cerebral organoid studies. The CB_1 receptor expression pattern in human cerebral organoids recapitulated the expression pattern observed *in vivo* during cortical development (Glass et al., 1997; Díaz-Alonso et al., 2012). CB_1 receptor expression was high in differentiated microtubule associate protein 2 (MAP2)-positive neurons. Moreover, CB_1 receptor expression was evident in deep and upper layer neurons, as identified by the expression of BCL11B and SATB2, respectively (Fig. 7A). Cerebral organoids were generated in the presence of the CB_1 receptors agonists HU-210 and THC (100 nM and 2 µM, respectively, from 30 to 60 DIV), and cortical layer development was characterized by immunofluorescence.

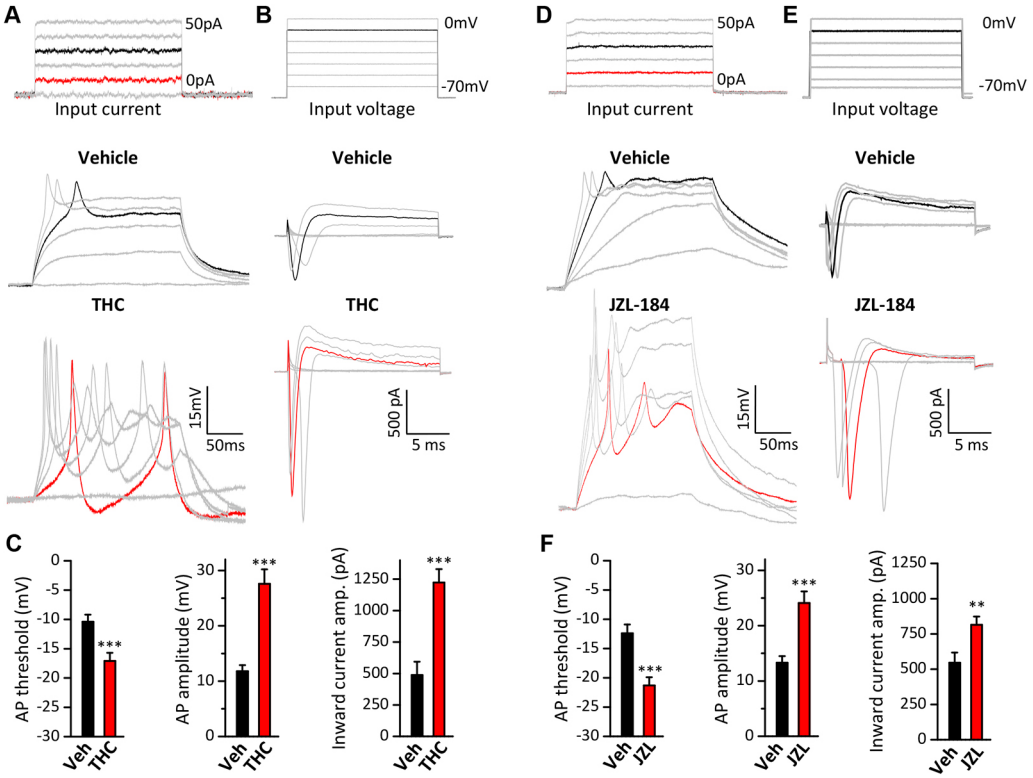

Fig. 6. THC and JZL-184 promote the acquisition of neuronal activity and maturation. (A-E) Mouse ES-cells differentiated in the presence of THC and JZL-148 were characterized by patch-clamp analyses. (A,D) Representative examples of the increasing currents (10 pA step) (top) injected in current-clamp recordings and the cell responses (bottom). Black and red traces correspond to the threshold injected current and the evoked action potential firing in vehicle- (black) and THC- or JZL-148- (red) differentiated cells, in vehicle- and THC- or JZL-148-differentiated cells. (B,E) Representative examples of series of increasing voltages (5 mV step) (top) and the cell responses (bottom). The black trace (top) shows the injected voltage (−10 mV) that evokes the highest inward current in the cell. Black and red traces (bottom) correspond to the inward current at −10 mV in vehicle- (black) and THC- or JZL-184- (red) differentiated cells. (C,F) Quantification of the change in the action potential threshold at −10 mM, action potential amplitude and inward current in THC- and JZL-184-differentiated neurons compared with vehicle-differentiated neurons. The analyses were done on THC- and JZL-184-derived neurons from n=4 and 3 differentiations, respectively. **P<0.01, ***P<0.001 (vs vehicle).

Development (2020) 147, dev192161. doi:10.1242/dev.192161

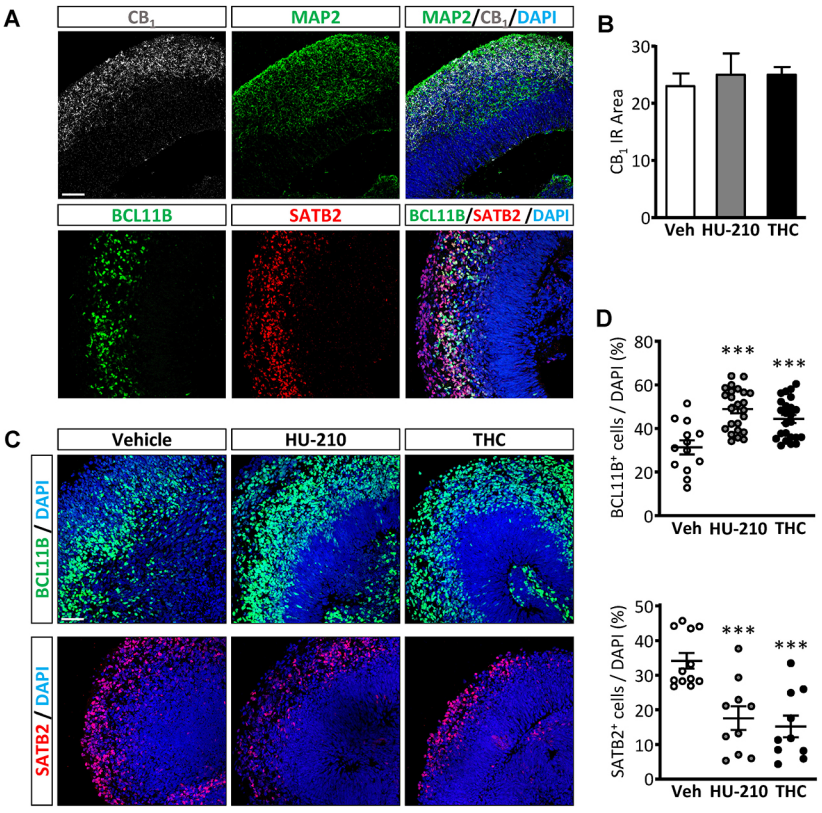

Fig. 7. Effect of CB_1 receptor activation on human iPS cell-derived organoids. (A) Cerebral organoids were characterized by immunofluorescence with anti-CB_1 receptor and anti-MAP2 antibodies (upper panels). Deep and upper cortical neurons were also analysed using specific antibodies for BCL11B and SATB2 (lower panels). (B) Organoids were treated with HU-210 (100 nM), THC (2 µM) or vehicle between 30 and 60 DIV. CB_1 receptor levels were quantified after immunofluorescence. (C,D) Representative images and quantification of BCL11B- and SATB2-neuronal generation after immunofluorescence. Analyses were done on n=3-7 ventricles, from a minimum of 4 cerebral organoids. ***P<0.001 (vs vehicle). Scale bar: 50 µm.

To determine the status of CB_1 receptors after differentiation in the presence of cannabinoid agonists, CB_1 immunoreactivity was quantified. CB_1 receptor levels in HU-210- and THC-differentiated organoids did not change in comparison with vehicle-treated organoids, suggesting the absence of CB_1 receptor desensitization (Fig. 7B). CB_1 receptor activation promoted the generation of $BCL11B^+$ deep layer neurons and reduced that of $SATB2^+$ upper layer neurons (Fig. 7C,D), thus recapitulating the findings derived from cannabinoid signalling manipulation during mouse ES cell-derived neuronal generation (present study) and mouse embryonic development (Díaz-Alonso et al., 2012).

DISCUSSION

In the present study we investigated the role of the eCB signalling system in ES-derived neuronal generation. We found that the overall expression of the different elements of the eCB system is induced along neuronal differentiation, and the levels of the endogenous ligands 2AG, AEA and other *N*-acylethanolamines are also increased. CB_1 receptor activation promoted deep layer cortical projection neuron generation and decreased upper layer neuronal development by regulating the transcription factors BCL11B and SATB2, with the possible participation of other identity determinants such as SKI. ES cell differentiation in the presence of the CB_1 receptor agonist THC or the MGL inhibitor JZL-184 promoted significant changes in electrophysiological parameters associated with neuronal maturation, as reflected in a decrease of the action potential threshold and an increase in the action potential amplitude (Zhang, 2004; Kroon et al., 2019). Hence, our findings identify a cell-autonomous role of eCB signalling, via CB_1 receptors, in ES-derived differentiation of pyramidal neurons, particularly by promoting the generation of deep layer cortical neurons. One limitation of our study is that the relative importance of cell-autonomous and paracrine actions of eCB signalling via CB_1 receptors in pyramidal neuronal differentiation may require further assessment using single cell transcriptomic analyses.

In the last decade, the contribution of eCB signalling to the modulation of neuronal differentiation and morphogenesis has been the object of intense research (Galve-Roperh et al., 2013; Maccarrone et al., 2014). Pharmacological manipulation of CB_1 receptor signalling by administration of THC (Alpár et al., 2014; Tortoriello et al., 2014; de Salas-Quiroga et al., 2015) or the SR-141716 antagonist (Mulder et al., 2008) has an impact on long-range projection neuron development as well as on acquisition of pyramidal intrinsic excitability (Bara et al., 2018). More conclusively, conditional CB_1 receptor loss of function in glutamatergic telencephalic neurons interferes with deep layer corticofugal and corticospinal motor neuron development (Mulder et al., 2008; Wu et al., 2010; Díaz-Alonso et al., 2012). In retinal neurons, CB_1 receptors regulate growth cone guidance, via crosstalk with DCC, controlling its membrane exposure in a PKA-dependent manner (Argaw et al., 2011). eCBs also regulate oligodendrocyte-derived Slit2, which, by acting over neuronal Robo1 receptors, influences on corticofugal neuron development (Alpár et al., 2014). The results herein demonstrate that the eCB system acts as a proneurogenic signalling system that, via CB_1 receptors, promotes the differentiation and maturation of deep layer pyramidal neurons (Díaz-Alonso et al., 2012; de Salas-Quiroga et al., 2015) by regulating the activity of BCL11B and SATB2 transcription factors. CB_1 receptor signalling favours *Bcl11b* transcriptional activity by alleviating SATB2-mediated repression via MAR sequences, and this allows the balanced expression of netrin1-mediated growth cone signalling receptors DCC and Unc5C (Srivatsa et al., 2014), hence contributing to the development of subcortical projection neurons. In addition, various *N*-acylethanolamine species have been proposed to act as inhibitors of Shh signalling acting on SMOOTHENED receptors, and independently of CB_1 and other

Development (2020) 147, dev192161. doi:10.1242/dev.192161

potential eCB receptors (CB_2, PPARα/γ, TRPV1) (Khaliullina et al., 2015), but the specific contribution of these mechanism to cortical development remains unexplored.

Our observations may also have implications regarding the impact of embryonic THC exposure and the risk of developing neuropsychiatric alterations and neurodevelopmental disorders (Alpár et al., 2016; Scheyer et al., 2019). Recent studies have used hiPS-derived neuronal generation as a useful tool for investigating the impact of THC on human development. Transcriptomic studies on hiPS-derived neurons exposed to THC revealed altered expression of genes involved in neurodevelopment and synaptic function, and a pattern that associates with neuropsychiatric conditions, particularly autism and intellectual disability (Guennewig et al., 2018). THC-treated hiPS cell-derived neurons showed attenuated transcriptional activity after KCl depolarization. In addition, THC exposure during adolescence induces developmental gene transcription changes associated with projection neuron maturation, dendritic maturation and psychiatric disorders (Miller et al., 2018). In a model of hiPS-derived neuronal generation, the presence of 2AG and THC negatively regulated neurite outgrowth, and this occurred in parallel with inhibition of the ERK and Akt pathways (Shum et al., 2020). Similarly, a recent report revealed that THC-treated hiPS cell-derived organoids possess reduced neuronal activity and neurite outgrowth (Ao et al., 2020). Hence, under these conditions, cannabinoid exposure probably induces CB_1 receptor desensitization and loss of function, rather than its activation (Ao et al., 2020; Shum et al., 2020). In a different neuronal lineage model, hiPS cell-derived dopaminergic neurons generated in the presence of THC and AEA were shown to display dual effects, with low cannabinoid concentrations exerting a positive effect on neuronal activity and high cannabinoid concentrations impairing activity (Stanslowsky et al., 2016). Considering the currently available evidence, it can be generally concluded that CB_1 receptor activity within a physiological range (that is not accompanied by receptor desensitization) promotes pyramidal neuron differentiation and maturation. Alternatively, pharmacological interference of cannabinoid signalling associated with CB_1 receptor loss of function exerts detrimental consequences on neuronal maturation. CB_1 receptor regulation of BCL11B deep layer pyramidal neuron differentiation was mediated by ERK and Akt signalling, but was independent of cAMP, mTORC1, JNK and proteasomal degradation. Hence, different signalling pathways are responsible for different CB_1 receptor-regulated neural cell fate processes. For example, CB_1 receptor-induced apical progenitor transition to basal progenitor cells relies on PI3K/Akt/mTORC1 signalling (Díaz-Alonso et al., 2015), whereas BCL11B neuronal differentiation is independent of mTORC1 activity and depends on ERK signalling (present report). Noteworthy, CB_1 receptor-driven CSMN differentiation is a postmitotic cell-dependent action, as demonstrated by the similar neuronal differentiation pattern in conditional Nex-CB_1 knockout mice and complete CB_1 knockout mice (Díaz-Alonso et al., 2012). ERK signalling is in turn essential in the development and acquisition of neuronal excitability of $BCL11B^+$ layer V neurons (Xing et al., 2016), hence providing further support for the role of CB_1 receptors in corticospinal motor neuron development and differentiation. Thus, eCB signalling-evoked regulation of neurogenesis relies on a delicate balance of CB_1 receptor actions by regulating cell proliferation and basal progenitor identity, which may affect final neuron number and direct or indirect neurogenesis (Díaz-Alonso et al., 2015) and neuronal differentiation (Díaz-Alonso et al., 2012; present study).

In the present study, the use of human cerebral organoids treated with THC and HU-210 provide further support for the involvement of CB_1 receptors in stem cell-derived neuronal generation and its modulatory role in the neuronal differentiation switch of deep layer versus upper layer neurons. Cerebral organoids generated in the presence of THC show alterations in progenitor proliferation (Ao et al., 2020) and upper layer development (present study). Similarly, *in vivo* THC administration alters projection neuron development and the balance between deep and upper layer development (de Salas-Quiroga et al., 2015; Bara et al., 2018). Importantly, alterations in the appropriate cortical layer-selective projection neuron development is altered in neuropsychiatric developmental diseases, including schizophrenia, autism and intellectual disability (Willsey et al., 2013; Ozair et al., 2018; Whitton et al., 2018). SATB2 is a genetic risk locus for schizophrenia, mental retardation and educational attainment (Whitton et al., 2018), and patients with mutations or deletions within the SATB2 locus experience severe learning difficulties and profound mental retardation (SATB2-associated syndrome) (Zarate and Fish, 2017). Likewise, pharmacologically induced overproduction of excitatory neurons in neocortical layer 2/3 recapitulates the development of autism-related traits (Fang et al., 2014), and correction of upper/deep layer projection neuron unbalance restores some of the behavioural autistic traits in a model of human 16p11.2 microdeletion (Pucilowska et al., 2012). Hence, the use of improved stem cell-derived neuron generation models opens new opportunities to understand the neurodevelopmental consequences of prenatal cannabinoid exposure (Alpár et al., 2016; Scheyer et al., 2019), as well as to unravel the contribution of the eCB system to neurodevelopmental diseases that result in severe neurological alterations (i.e. refractory epilepsy) (Soltesz et al., 2015; Cristino et al., 2020) and neuropsychiatric disorders (Fernández-Ruiz et al., 2020).

In summary, this study demonstrates a functional role of the eCB system in ES cell-derived neuronal generation and sheds light on the intracellular signalling mechanisms responsible for CB_1 receptor regulation of BCL11B-mediated pyramidal neuronal differentiation. Moreover, our findings show that, during ES neuronal differentiation, CB_1 receptor signalling promotes deep layer pyramidal neuron development and maturation, and this proneurogenic action can be manipulated pharmacologically, either directly by THC or other CB_1 agonists, or indirectly by inhibiting MGL and increasing 2AG levels.

MATERIALS AND METHODS

Materials

All reagents, unless otherwise indicated, were from Sigma-Aldrich (St Louis, MO). AM-251 and JZL-184 (Tocris, Bristol, UK), UO126 (Santa Cruz, Dallas, TX), Akt inhibitor X (Calbiochem, San Diego, CA), rapamycin (Tecoland Corporation, Irvine, CA) and THC (≥99% HPLC; THC Pharm, Frankfurt am Main, Germany) were used. The following materials were kindly donated: luciferase construct with MAR sequence A4 of the *Bcl11b* promoter (R. Grosschedl, Max-Planck-Institute of Immunobiology and Epigenetics, Freiburg, Germany), MAR3 and MAR2-luciferase constructs of the *Dcc* promoter (V. Tarabykin, Charité Universitäts Medizin Berlin, Germany) and HU-210 (R. Mechoulam, Hebrew University, Jerusalem, Israel).

Mouse ES cell culture and neuronal differentiation

The R1 mouse embryonic stem (mES) cell line (kindly donated by UFIEC, ISCIII, Madrid, Spain) was employed after neural induction and differentiation in the absence of morphogens and in the presence of cyclopamine (Sigma-Aldrich) (Gaspard et al., 2008). R1 cells were grown on 0.1% gelatin in ES medium containing Knockout Dulbecco's modified Eagle medium (DMEM) (Gibco, Carlsbad, CA) supplemented with 20% Knockout Serum Replacement (Gibco), 1000 U/ml leukemia inhibitory

Development (2020) 147, dev192161. doi:10.1242/dev.192161

factor (Millipore, Burlington, MA), 0.1 mM non-essential amino acids (Lonza, Basel, Switzerland), 2 mM ultraglutamine (Lonza), 50 U/ml penicillin and streptomycin (Lonza) and 0.1 mM 2-mercaptoethanol (Gibco). For mES differentiation, cells were plated at low density (5000 cells/cm^2) in ES medium for 1 day. Then, the medium was changed to Defined Default Medium (DDM) containing DMEM/F12+GlutaMAX (Gibco) with N2 supplement (Millipore) (1×), 5 mM HEPES buffer (Lonza), 0.1 mM non-essential amino acids (Lonza), 1 mM sodium pyruvate (Lonza), 2.5 mg/ml AlbuMax-I (Gibco), 30 mM D-glucose (Sigma-Aldrich), 0.1 mM 2-mercaptoethanol (Gibco) and 50 U/ml penicillin and streptomycin (Lonza) and cells cultured for 12 days. Cells were trypsinized, dissociated gently and filtered through 100 µm filter to discard cell aggregates. Cells were then plated (100,000 cells/cm^2) on polylysine/laminin (Sigma-Aldrich)-coated dishes in 50% DDM and 50% Neurobasal supplemented with B27 (Gibco) (without vitamin A, 1×), 2 mM ultraglutamine (Lonza) and 50 U/ml penicillin and streptomycin (Lonza) and cultured for 9 days. Cannabinoid treatment was performed during neuronal differentiation, between days 14 and 21, and culture medium was renewed every 2 days. Preliminary dose-dependency studies were performed in order to determine the most appropriate ligand concentrations for pharmacological manipulation. Lack of cell death was determined by immunofluorescence with anti-cleaved-caspase 3 antibody (see Fig. S7). Cell lines were routinely analysed for contamination and mycoplasma screening.

The expression of pluripotency, neural stem and neuronal markers was monitored by real time PCR and immunofluorescence to follow pluripotent ES transition to the NS cell state (12 DIV) and neurons (21 DIV). CB_1 receptor knockdown was performed in R1 mES cells with 10 µg pGFP-V-RS (Origene, Rockville, MD) encoding shCtrl or shCB_1 nucleofection using Amaxa Nucleofector (AAB-1001, Lonza, program A-013, 5×10^6 cells). Positive colonies were selected using puromycin (Sigma-Aldrich) and dissociated cells were cultured as described above. In some experiments, R1-derived NS cells were employed. Transfection was performed at 14 DIV using Lipofectamine 2000 (ThermoFisher Scientific) following the manufacturer's instructions. NS cells were seeded in 12-well plates, transiently transfected with 1.5 µg shCtrl or shCB1 pGFP-V-RS (Origene) and analysed at 21 DIV.

For CB_1 receptor expression rescue, a shRNA-resistant form of human CB_1 receptor was inserted into pcDNA3.1 with an N-terminus 3×FLAG. At 14 DIV, pcDNA or pcDNA-CB_1 transfection in shCtrl-R1 or shCB_1-R1 cells was performed using Lipofectamine 2000 (ThermoFisher Scientific). Cells were subsequently analysed at 21 DIV.

Immunofluorescence characterization

Immunofluorescence was performed, after blockade with 5% goat serum, by overnight incubation at 4°C with the indicated primary antibodies (Table S2), followed by incubation for 1 h at room temperature with secondary antibodies. The appropriate anti-mouse, rat, guinea pig and rabbit highly cross-adsorbed Alexa Fluor 488, Alexa Fluor 594 and Alexa Fluor 647 secondary antibodies (ThermoFisher Scientific, Waltham, MA) were used. Confocal fluorescence images were acquired using LAS-X software with a SP8 microscope, with three passes by Kalman filter and a 1024×1024 collection box. Immunofluorescence data were obtained in a blinded manner; quantifications were obtained in 6-8 fields (250 cells/field) from the indicated number (*n*) of independent experiments.

Luciferase transcriptional assays and gene expression analyses

To study BCL11B transcriptional activity, R1 and HiB5 cells (kindly provided by Z. Kokaia, Lund University, Sweden) were seeded on 24-well plates and transiently co-transfected with 2 µg of the luciferase reporter vector matrix attachment region (MAR)-A4-pfosluc reporter of *Bcl11b* promoter (Díaz-Alonso et al., 2012) or MAR1-pfosluc of *Dcc* promoter (Vector Builder, Neu-Isenburg, Germany), using Lipofectamine 2000 (ThermoFisher Scientific) following the manufacturer's instructions. To correct for transfection efficacy, 200 ng *Renilla* luciferase (pRL-CMV) was also co-transfected. For *Bcl11b* and *Dcc* gene regulation assays, preliminary experiments were performed with luciferase reporters of MAR-A4, MAR-A3 and MAR3, MAR2, MAR1 sequences, respectively. MAR-A4-*Bcl11b* and MAR1-*Dcc* were the best responders to CB_1 receptor regulation and selected for further studies. After stimulation, the luciferase activities were quantified using the Dual-Luciferase Reporter assay system (Promega Madison, WI) in a Lumat LB9507 luminometer (Berthold Technologies, Bad Wildbad, Germany).

Real-time quantitative PCR

RNA was isolated using RNeasy Plus kit (Quiagen, Hilden, Germany). cDNA was obtained with Transcriptor (Roche, Basel, Switzerland). Real-time qPCR assays were performed using the FastStart Master Mix with Rox (Roche) and probes were obtained from the Universal Probe Library Set (Roche). Amplifications were run in a 7900 HT-Fast Real-Time PCR System (Applied Biosystems, Waltham, MA). Each value was adjusted by using 18S, TATA-box-binding protein and β-actin RNA levels as reference. The primers used are indicated in Table S3.

Electrophysiology experiments

Control, THC- and JZL-184-derived neurons were transferred to an immersion recording chamber and superfused at 1 ml/min with an external solution containing (in mM) 125 NaCl, 1 $MgCl_2$•$6H_2O$, 3 $CaCl_2$•$2H_2O$, 2.5 KCl, 10 HEPES, and 20 glucose (pH 7.3, osmolality 280–290 mOsm/l) (Verma et al., 2017). Patch-clamp analyses were performed according to standard protocols as previously described (Martín et al., 2018). Experiments were performed at 25°C using a temperature controller (Warner Instruments). Neurons possessing pyramidal-shaped somas with long neurites were identified for recordings by observation under a 40× water immersion objective and a Nomarski condenser combined with infrared microscopy using differential interface contrast (DIC) in an Eclipse FN1 Nikon microscope. Whole-cell electrophysiological recordings were performed using patch pipettes (3-5 MΩ resistance) pulled from thick-walled borosilicate glass (1.5 mm outer and 1.1 mm inner diameter) on a P-97 puller (Sutter-Instrument) and filled with the internal solution containing (in mM) 135 potassim gluconate, 10 KCl, 10 HEPES, 1 $MgCl_2$, 2 ATP-Na_2 (pH 7.3 adjusted with KOH; osmolality 280–290 mOsm/l). In some experiments, 5 mM biocytin (Tocris) was added to the internal solution for *post-hoc* analysis of neuronal identity by immunofluorescence. After formation of a whole-cell configuration (–70 mV holding potential), current- or voltage-clamp protocols were applied. For the voltage-clamp recordings, a series of increasing voltages (5 mV step, 50 ms duration with a 3 s interval) were injected. For the current-clamp recordings, a series of increasing currents (10 pA step, 100 ms duration with a 3 s interval) were injected. Recordings were obtained by a PC-ONE amplifier, and signals were fed to a Pentium-based PC through a DigiData1322A interface board. pCLAMP 10.2 software was used for stimulus generation, data display, acquisition, storage and analysis.

Immunoblot assays

Protein extracts were prepared in radioimmunoprecipitation assay (RIPA) lysis buffer supplemented with protease inhibitors. Samples were heated at 37°C for 15 min. Equal amounts of protein samples were electrophoretically separated and transferred to PDVF membranes. After blocking with 5% BSA, membranes were incubated overnight at 4°C with the indicated primary antibodies (Table S2). Then, membranes were incubated with the corresponding secondary antibodies coupled to horseradish peroxidase for 1 h at room temperature and revealed with enhanced chemiluminescence (ECL, Biorad, Hercules, CA). The optical density of the relevant immunoreactive bands was quantified with ImageJ software and normalized to β-actin for the corresponding samples in the same membranes.

Human iPS cell culture and cerebral organoid differentiation

Experiments with human induced pluripotent stem (hiPS) cells were conducted in the Max Planck Institute of Psychiatry (Munich, Germany). hiPS cells were maintained on Geltrex-coated dishes (ThermoFisher Scientific) in human ES medium containing mTesR1 medium and mTesR1 supplement (1×; Stem Cell Technologies, Vancouver, Canada). Cells were passed after 5 min Accutase (Sigma-Aldrich) treatment. For

cerebral organoid differentiation (Klaus et al., 2019; Buchsbaum et al., 2020), 9000 cells/well were plated on ultralow attachment 96-well plates (Corning, NY) in human ES medium with low concentration basic fibroblast growth factor (4 ng/ml; Peprotech, Rocky Hill, NJ) and 50 µM Rho-associated protein kinase (ROCK) inhibitor (Stem Cell Technologies). Embryoid bodies were maintained for 6 days and then transferred to ultralow attachment 24-well plates (Corning) in neural induction media containing DMEM/F12+Glutamax (Gibco), N2 supplement (1:100; Gibco), minimum essential media-nonessential amino acids (MEM-NEAA) (1:100; Gibco) and heparin (1 µg/ml, Sigma-Aldrich) for 5 days. On day 12, neuroepithelial tissues formed and were transferred to Matrigel droplets (Corning) and grown in differentiation medium containing 50% DMEM/F12+Glutamax and 50% Neurobasal containing N2 supplement (1:200; Gibco), B27 supplement without vitamin A (1:100; Gibco), 0.1 mM 2-mercaptoethanol (Gibco), insulin (1:4000; Sigma), MEM-NEAA (1:200; Gibco) and antibiotic-antimycotic solution (1:100; Gibco). After 4 days of stationary growth, organoids were kept in dishes on an orbital shaker at 37°C and 5% CO_2 in differentiation medium containing B27 supplement with vitamin A (Gibco). Organoids were analysed after cannabinoid treatment between 30 and 60 DIV, with medium changes every 3 days. Cannabinoid concentrations used for pharmacological regulation of organoid development were characterized in preliminary dose-dependent studies. The lack of toxicity was assessed by determination of organoid area, morphology and cell death with anti-cleaved-caspase 3 antibody (see Fig. S7). The doses of 100 nM HU-210 and 2 µM THC were finally selected. For immunofluorescence studies in cerebral organoids, 18 µm sections of organoids were prepared using a cryostat, and every tenth section was collected onto a slide to obtain ten slides containing serial sections representing the whole organoid. Immunostaining was performed as described previously (Buchsbaum et al., 2020). For quality control and selection of ventricles with dorsal identity to include in the analyses, sections were stained for BCL11B and SATB2. Analysis was conducted in 12 and 10-24 different ventricles (vehicle and HU-210 or THC, respectively) in a total of 4 and 4-7 organoids (vehicle and HU-210 or THC, respectively). Images were acquired in sequential xyz mode with at least 1024×1024 pixels and 0.8-1.2 µm thickness of optical z-layers. Image analysis was conducted in Fiji; single cells were counted using the manual cell counter plugin on a single image of the z-stack. For quantification of neurons upon treatment, all $BCL11B^+$ and $SATB2^+$ cells in the corresponding ventricle were counted and related to the total number of $DAPI^+$ cells inside the ventricle.

Determination of endocannabinoid levels

eCBs levels were measured in cell extracts from proliferating and differentiated R1 cells as described (Lomazzo et al., 2015) by the Endocannabinoids Lipidomics Group (Institute Physiological Chemistry, University Medical Center Mainz, Mainz, Germany).

Data analyses and statistics

Results shown represent the means±s.e.m., and the number of experiments is indicated in every case. For multiple comparisons, statistical analysis was performed by one-way ANOVA, with a *post-hoc* analysis made using Fisher's LSD test. For analysis of two independent groups, an unpaired Student's *t*-test or Welch's test was performed, as appropriate. Analysis was done using GraphPad Prism 8.0 (GraphPad Software, La Jolla, CA). Detailed statistical analyses are provided in Table S4.

Acknowledgements

We are grateful to R. Bajo-Grañeras (Complutense University, Spain) for technical advice, and to C. Utrilla (Complutense University, Spain) and S. Mylonas (Athens University, Greece) for assistance with preliminary experiments.

Competing interests

The authors declare no competing or financial interests.

Author contributions

Conceptualization: I.G.-R.; Methodology: J.P.-L., J.A., R.M., A.C.A.-M., D.G.-R., A.d.S.-Q., J.S.-P., S.C., I.G.-R.; Validation: J.P.-L., J.A.; Formal analysis: J.P.-L., J.A., R.M., S.S.-S., D.G.-R., C.C.-I., A.d.S.-Q., J.D.-A., I.L., I.G.-R.; Investigation: J.P.-L., J.A., R.M., A.C.A.-M., S.S.-S., D.G.-R., C.C.-I., E.G.-T., A.d.S.-Q., J.D.-A., I.L.; Resources: M.G., I.G.-R.; Data curation: J.P.-L.; Writing - original draft: I.G.-R.; Writing - review & editing: J.P.-L., S.C., M.G., I.G.-R.; Visualization: J.P.-L., I.G.-R.; Supervision: J.S.-P., S.C., M.G., I.G.-R.; Project administration: I.G.-R.; Funding acquisition: M.G., I.G.-R.

Funding

This work was supported by the European Regional Development Fund 'A way to achieve Europe' (PI18-00941 to I.G.-R., RTI2018-095311-B-100 to M.G., BFU2017-83292-R to J.S.-P. and RTI2018-101663-B-100 to I.L.). J.P.-L., J.A. and S.S.-S., were supported by FPU, FPI and PFIS program fellowships, respectively, from the Ministerio de Educación, Cultura y Deporte, Ministerio de Ciencia and Ministerio de Sanidad. S.S.-S. was also supported by the Fondo Social Europeo-La Iniciativa sobre Empleo Juvenil (YEI) (CT101/18-CT102/18PEJD-2018-PRE/BMD-7933). A.d.S.-Q., D.G.-R. and R.M. were supported by the Centro de Investigación Biomédica en Red sobre Enfermedades Neurodegenerativas (CIBERNED), Fundación Tatiana Pérez de Guzmán el Bueno and European Regional Development Fund (BFU2017-83292-R), respectively.

Data availability

The raw data have been deposited in Dryad (https://doi.org/10.5061/dryad.h9w0vt4g9).

Supplementary information

Supplementary information available online at
https://dev.biologists.org/lookup/doi/10.1242/dev.192161.supplemental

Peer review history

The peer review history is available online at
https://dev.biologists.org/lookup/doi/10.1242/dev.192161.reviewer-comments.pdf

References

Alcamo, E. A., Chirivella, L., Dautzenberg, M., Dobreva, G., Fariñas, I., Grosschedl, R. and Mcconnell, S. K. (2008). Satb2 regulates callosal projection neuron identity in the developing cerebral cortex. *Neuron* **57**, 364-377. doi:10.1016/j.neuron.2007.12.012

Alpár, A., Tortoriello, G., Calvigioni, D., Niphakis, M. J., Milenkovic, I., Bakker, J., Cameron, G. A., Hanics, J., Morris, C. V., Fuzik, J. et al. (2014). Endocannabinoids modulate cortical development by configuring Slit2/Robo1 signalling. *Nat. Commun.* **5**, 4421. doi:10.1038/ncomms5421

Alpár, A., Di Marzo, V. and Harkany, T. (2016). At the tip of an iceberg: prenatal marijuana and its possible relation to neuropsychiatric outcome in the offspring. *Biol. Psychiatry* **79**, e33-e45. doi:10.1016/j.biopsych.2015.09.009

Ao, Z., Cai, H., Havert, D. J., Wu, Z., Gong, Z., Beggs, J. M., Mackie, K. and Guo, F. (2020). One-stop microfluidic assembly of human brain organoids to model prenatal cannabis exposure. *Anal Chem.* **92**, 4630-4638. doi:10.1101/2020.01.15.908483

Argaw, A., Duff, G., Zabouri, N., Cécyre, B., Chainé, N., Cherif, H., Tea, N., Lutz, B., Ptito, M. and Bouchard, J.-F. (2011). Concerted action of CB1 cannabinoid receptor and deleted in colorectal cancer in axon guidance. *J. Neurosci.* **31**, 1489-1499. doi:10.1523/JNEUROSCI.4134-09.2011

Bara, A., Manduca, A., Bernabeu, A., Borsoi, M., Serviado, M., Lassalle, O., Murphy, M., Wager-Miller, J., Mackie, K., Pelissier-Alicot, A.-L. et al. (2018). Sex-dependent effects of in utero cannabinoid exposure on cortical function. *eLife* **7**, e36234. doi:10.7554/eLife.36234.025

Baranek, C., Dittrich, M., Parthasarathy, S., Bonnon, C. G., Britanova, O., Lanshakov, D., boukhtouche, F., Sommer, J. E., Colmenares, C., Tarabykin, V. et al. (2012). Protooncogene Ski cooperates with the chromatin-remodeling factor Satb2 in specifying callosal neurons. *Proc. Natl. Acad. Sci. USA* **109**, 3546-3551. doi:10.1073/pnas.1108718109

Berghuis, P., Dobszay, M. B., Wang, X., Spano, S., Ledda, F., Sousa, K. M., Schulte, G., Ernfors, P., Mackie, K., Paratcha, G. et al. (2005). Endocannabinoids regulate interneuron migration and morphogenesis by transactivating the TrkB receptor. *Proc. Natl. Acad. Sci. USA* **102**, 19115-19120. doi:10.1073/pnas.0509494102

Buchsbaum, I. Y., Kielkowski, P., Giorgio, G., O'Neill, A. C., Di Giaimo, R., Kyrousi, C., Khattak, S., Sieber, S. A., Robertson, S. P. and Cappello, S. (2020). ECE2 regulates neurogenesis and neuronal migration during human cortical development. *EMBO Rep.* **21**, e48204. doi:10.15252/embr.201948204

Cristino, L., Bisogno, T. and Di Marzo, V. (2020). Cannabinoids and the expanded endocannabinoid system in neurological disorders. *Nat. Rev. Neurol.* **16**, 9-29. doi:10.1038/s41582-019-0284-z

de Salas-Quiroga, A., Díaz-Alonso, J., García-Rincón, D., Remmers, F., Vega, D., Gómez-Cañas, M., Lutz, B., Guzmán, M. and Galve-Roperh, I. (2015). Prenatal exposure to cannabinoids evokes long-lasting functional alterations by targeting CB_1 receptors on developing cortical neurons. *Proc. Natl. Acad. Sci. USA* **112**, 13693-13698. doi:10.1073/pnas.1514962112

de Salas-Quiroga, A., García-Rincón, D., Gómez-Domínguez, D., Valero, M., Simón-Sánchez, S., Paraíso-Luna, J., Aguareles, J., Pujadas, M., Muguruza, C., Callado, L. F. et al. (2020). Long-term hippocampal interneuronopathy drives sex-dimorphic spatial memory impairment induced by prenatal THC exposure. *Neuropsychopharmacology* **45**, 877-886. doi:10.1038/s41386-020-0621-3

Díaz-Alonso, J., Aguado, T., Wu, C.-S., Palazuelos, J., Hofmann, C., Garcez, P., Guillemot, F., Lu, H.-C., Lutz, B., Guzman, M. et al. (2012). The CB(1) cannabinoid receptor drives corticospinal motor neuron differentiation through the Ctip2/Satb2 transcriptional regulation axis. *J. Neurosci.* **32**, 16651-16665. doi:10.1523/JNEUROSCI.0681-12.2012

Díaz-Alonso, J., Aguado, T., De Salas-Quiroga, A., Ortega, Z., Guzmán, M. and Galve-Roperh, I. (2015). CB1 cannabinoid receptor-dependent activation of mTORC1/Pax6 signaling drives Tbr2 expression and basal progenitor expansion in the developing mouse cortex. *Cereb. Cortex* **25**, 2395-2408. doi:10.1093/cercor/bhu039

Díaz-Alonso, J., De Salas-Quiroga, A., Paraíso-Luna, J., García-Rincón, D., Garcez, P. P., Parsons, M., Andradas, C., Sánchez, C., Guillemot, F., Guzmán, M., et al. (2017). Loss of cannabinoid CB1Receptors induces cortical migration malformations and increases seizure susceptibility. *Cereb. Cortex* **27**, 5303-5317. doi:10.1093/cercor/bhw309

Fang, W.-Q., Chen, W.-W., Jiang, L., Liu, K., Yung, W.-H., Fu, A. K. Y. and Ip, N. Y. (2014). Overproduction of upper-layer neurons in the neocortex leads to autism-like features in mice. *Cell Rep.* **9**, 1635-1643. doi:10.1016/j.celrep.2014.11.003

Fernández-Ruiz, J., Galve-Roperh, I., Sagredo, O. and Guzmán, M. (2020). Possible therapeutic applications of cannabis in the neuropsychopharmacology field. *Eur. Neuropsychopharmacol.* **36**, 217-234. doi:10.1016/j.euroneuro.2020.01.013

Frau, R., Miczán, V., Traccis, F., Aroni, S., Pongor, C. I., Saba, P., Serra, V., Sagheddu, C., Fanni, S., Congiu, M. et al. (2019). Prenatal THC exposure produces a hyperdopaminergic phenotype rescued by pregnenolone. *Nat. Neurosci.* **22**, 1975-1985. doi:10.1038/s41593-019-0512-2

Galve-Roperh, I., Chiurchiù, V., Díaz-Alonso, J., Bari, M., Guzmán, M. and Maccarrone, M. (2013). Cannabinoid receptor signaling in progenitor/stem cell proliferation and differentiation. *Prog. Lipid Res.* **52**, 633-650. doi:10.1016/j.plipres.2013.05.004

Gaspard, N., Bouschet, T., Hourez, R., Dimidschstein, J., Naeije, G., Van Den Ameele, J., Espuny-Camacho, I., Herpoel, A., Passante, L., Schiffmann, S. N. et al. (2008). An intrinsic mechanism of corticogenesis from embryonic stem cells. *Nature* **455**, 351-357. doi:10.1038/nature07287

Glass, M., Dragunow, M. and Faull, R. L. M. (1997). Cannabinoid receptors in the human brain: a detailed anatomical and quantitative autoradiographic study in the fetal, neonatal and adult human brain. *Neuroscience* **77**, 299-318. doi:10.1016/S0306-4522(96)00428-9

Greig, L. C., Woodworth, M. B., Galazo, M. J., Padmanabhan, H. and Macklis, J. D. (2013). Molecular logic of neocortical projection neuron specification, development and diversity. *Nat. Rev. Neurosci.* **14**, 755-769. doi:10.1038/nrn3586

Guennewig, B., Bitar, M., Obiorah, I., Hanks, J., O'Brien, E. A., Kaczorowski, D. C., Hurd, Y. L., Roussos, P., Brennand, K. J. and Barry, J. (2018). THC exposure of human iPSC neurons impacts genes associated with neuropsychiatric disorders. *Transl. Psychiatry* **8**, 89. doi:10.1038/s41398-018-0137-3

Khaliullina, H., Bilgin, M., Sampaio, J. L., Shevchenko, A. and Eaton, S. (2015). Endocannabinoids are conserved inhibitors of the hedgehog pathway. *Proc. Natl. Acad. Sci. USA* **112**, 3415-3420. doi:10.1073/pnas.1416463112

Klaus, J., Kanton, S., Kyrousi, C., Ayo-Martin, A. C., Di Giaimo, R., Riesenberg, S., O'Neill, A. C., Camp, J. G., Tocco, C., Santel, M. et al. (2019). Altered neuronal migratory trajectories in human cerebral organoids derived from individuals with neuronal heterotopia. *Nat. Med.* **25**, 561-568. doi:10.1038/s41591-019-0371-0

Kroon, T., Van Hugte, E., Van Linge, L., Mansvelder, H. D. and Meredith, R. M. (2019). Early postnatal development of pyramidal neurons across layers of the mouse medial prefrontal cortex. *Sci. Rep.* **9**, 5037. doi:10.1038/s41598-019-41661-9

Lomazzo, E., Bindila, L., Remmers, F., Lerner, R., Schwitter, C., Hoheisel, U. and Lutz, B. (2015). Therapeutic potential of inhibitors of endocannabinoid degradation for the treatment of stress-related hyperalgesia in an animal model of chronic pain. *Neuropsychopharmacology* **40**, 488-501. doi:10.1038/npp.2014.198

Maccarrone, M., Guzmán, M., Mackie, K., Doherty, P. and Harkany, T. (2014). Programming of neural cells by (endo)cannabinoids: from physiological rules to emerging therapies. *Nat. Rev. Neurosci.* **15**, 786-801. doi:10.1038/nrn3846

Martín, R., Ferrero, J. J., Collado-Alsina, A., Aguado, C., Luján, R., Torres, M. and Sánchez-Prieto, J. (2018). Bidirectional modulation of glutamatergic synaptic transmission by metabotropic glutamate type 7 receptors at Schaffer collateral–CA1 hippocampal synapses. *J. Physiol.* **596**, 921-940. doi:10.1113/JP275371

Miller, M. L., Chadwick, B., Dickstein, D. L., Purushothaman, I., Egervari, G., Rahman, T., Tessereau, C., Hof, P. R., Roussos, P., Shen, L. et al. (2018). Adolescent exposure to Δ9-tetrahydrocannabinol alters the transcriptional trajectory and dendritic architecture of prefrontal pyramidal neurons. *Mol. Psychiatry* **24**, 588-600. doi:10.1038/s41380-018-0243-x

Mulder, J., Aguado, T., Keimpema, E., Barabás, K., Ballester Rosado, C. J., Nguyen, L., Monory, K., Marsicano, G., Di Marzo, V., Hurd, Y. L. et al. (2008). Endocannabinoid signaling controls pyramidal cell specification and long-range axon patterning. *Proc. Natl. Acad. Sci. USA* **105**, 8760-8765. doi:10.1073/pnas.0803545105

Ozair, M. Z., Kirst, C., van Den Berg, B. L., Ruzo, A., Rito, T. and Brivanlou, A. H. (2018). hPSC modeling reveals that fate selection of cortical deep projection neurons occurs in the subplate. *Cell Stem Cell* **23**, 60-73.e6. doi:10.1016/j.stem.2018.05.024

Pucilowska, J., Puzerey, P. A., Karlo, J. C., Galan, R. F. and Landreth, G. E. (2012). Disrupted ERK signaling during cortical development leads to abnormal progenitor proliferation, neuronal and network excitability and behavior, modeling human neuro-cardio-facial-cutaneous and related syndromes. *J. Neurosci.* **32**, 8663-8677. doi:10.1523/JNEUROSCI.1107-12.2012

Renard, J., Rosen, L. G., Loureiro, M., De Oliveira, C., Schmid, S., Rushlow, W. J. and Laviolette, S. R. (2017). Adolescent cannabinoid exposure induces a persistent sub-cortical hyper-dopaminergic state and associated molecular adaptations in the prefrontal cortex. *Cereb. Cortex* **27**, 1297-1310. doi:10.1093/cercor/bhv335

Sagredo, O., Palazuelos, J., Gutierrez-Rodriguez, A., Satta, V., Galve-Roperh, I. and Martínez-Orgado, J. (2018). Cannabinoid signalling in the immature brain: encephalopathies and neurodevelopmental disorders. *Biochem. Pharmacol.* **157**, 85-96. doi:10.1016/j.bcp.2018.08.014

Scheyer, A. F., Melis, M., Trezza, V. and Manzoni, O. J. J. (2019). Consequences of perinatal cannabis exposure. *Trends Neurosci.* **42**, 871-884. doi:10.1016/j.tins.2019.08.010

Shum, C., Dutan, L., Annuario, E., Warre-Cornish, K., Taylor, S. E., Taylor, R. D., Andreae, L. C., Buckley, N. J., Price, J., Bhattacharyya, S. et al. (2020). Δ9-tetrahydrocannabinol and 2-AG decreases neurite outgrowth and differentially affects ERK1/2 and Akt signaling in hiPSC-derived cortical neurons. *Mol. Cell. Neurosci.* **103**, 103463. doi:10.1016/j.mcn.2019.103463

Soltesz, I., Alger, B. E., Kano, M., Lee, S.-H., Lovinger, D. M., Ohno-Shosaku, T. and Watanabe, M. (2015). Weeding out bad waves: Towards selective cannabinoid circuit control in epilepsy. *Nat. Rev. Neurosci.* **16**, 264-277. doi:10.1038/nrn3937

Srivatsa, S., Parthasarathy, S., Britanova, O., Bormuth, I., Donahoo, A.-L., Ackerman, S. L., Richards, L. J. and Tarabykin, V. (2014). Unc5C and DCC act downstream of Ctip2 and Satb2 and contribute to corpus callosum formation. *Nat. Commun.* **5**, 3708. doi:10.1038/ncomms4708

Stanslowsky, N., Jahn, K., Venneri, A., Naujock, M., Haase, A., Martin, U., Frieling, H. and Wegner, F. (2016). Functional effects of cannabinoids during dopaminergic specification of human neural precursors derived from induced pluripotent stem cells. *Addict. Biol.* **22**, 1329-1342. doi:10.1111/adb.12394

Tortoriello, G., Morris, C. V., Alpar, A., Fuzik, J., Shirran, S. L., Calvigioni, D., Keimpema, E., Botting, C. H., Reinecke, K., Herdegen, T. et al. (2014). Miswiring the brain: Δ9-tetrahydrocannabinol disrupts cortical development by inducing an SCG10/stathmin-2 degradation pathway. *EMBO J.* **33**, 668-685. doi:10.1002/embj.201386035

Vargish, G. A., Pelkey, K. A., Yuan, X., Chittajallu, R., Collins, D., Fang, C. and McBain, C. J. (2016). Persistent inhibitory circuit defects and disrupted social behaviour following in utero exogenous cannabinoid exposure. *Mol. Psychiatry* **22**, 56-67. doi:10.1038/mp.2016.17

Verma, I., Rashid, Z., Sikdar, S. K. and Seshagiri, P. B. (2017). Efficient neural differentiation of mouse pluripotent stem cells in a serum-free medium and development of a novel strategy for enrichment of neural cells. *Int. J. Dev. Neurosci.* **61**, 112-124. doi:10.1016/j.ijdevneu.2017.06.009

Wei, D., Allsop, S., Tye, K. and Piomelli, D. (2017). Endocannabinoid Signaling in the Control of Social Behavior. *Trends Neurosci.* **40**, 385-396. doi:10.1016/j.tins.2017.04.005

Whitton, L., Apostolova, G., Rieder, D., Dechant, G., Rea, S., Donohoe, G. and Morris, D. W. (2018). Genes regulated by SATB2 during neurodevelopment contribute to schizophrenia and educational attainment. *PLoS Genet.* **14**, e1007515. doi:10.1371/journal.pgen.1007515

Willsey, A. J., Sanders, S. J., Li, M., Dong, S., Tebbenkamp, A. T., Muhle, R. A., Reilly, S. K., Lin, L., Fertuzinhos, S., Miller, J. A. et al. (2013). Coexpression networks implicate human midfetal deep cortical projection neurons in the pathogenesis of autism. *Cell* **155**, 997. doi:10.1016/j.cell.2013.10.020

Wu, C.-S., Zhu, J., Wager-Miller, J., Wang, S., O'leary, D., Monory, K., Lutz, B., Mackie, K. and Lu, H.-C. (2010). Requirement of cannabinoid CB(1) receptors in cortical pyramidal neurons for appropriate development of corticothalamic and thalamocortical projections. *Eur. J. Neurosci.* **32**, 693-706. doi:10.1111/j.1460-9568.2010.07337.x

Xing, L., Larsen, R. S., Bjorklund, G. R., Li, X., Wu, Y., Philpot, B. D., Snider, W. D. and Newbern, J. M. (2016). Layer specific and general requirements for ERK/MAPK signaling in the developing neocortex. *eLife* **5**, e11123. doi:10.7554/eLife.11123

Zarate, Y. A. and Fish, J. L. (2017). SATB2-associated syndrome: Mechanisms, phenotype, and practical recommendations. *Am. J. Med. Genet. Part A* **173**, 327-337. doi:10.1002/ajmg.a.38022

Zhang, Z.-W. (2004). Maturation of layer V pyramidal neurons in the rat prefrontal cortex: intrinsic properties and synaptic function. *J. Neurophysiol.* **91**, 1171-1182. doi:10.1152/jn.00855.2003